sustainability

MDPI

Article

Co-Gasification Performance of Low-Quality Lignite with Woody Wastes Using Greenhouse Gas CO_2—A TG–MS Study

Despina Vamvuka *, George Tsagris and Christia Loulashi

School of Mineral Resources Engineering, Technical University of Crete, 73100 Chania, Greece; giorgostsagris6@gmail.com (G.T.); christia1998c@yahoo.gr (C.L.)
* Correspondence: vamvuka@mred.tuc.gr

Abstract: The carbon dioxide gasification performance of low-quality lignite-agroindustrial/forest waste blends was investigated in terms of reactivity, conversion, cold gas efficiency, product gas composition and heating value. The experiments were conducted in a fixed bed unit and a thermal analysis mass spectrometer system. Raw materials, chars, liquids and gases were quantitatively analyzed and their energy content was determined. Synergetic effects and the role of minerals were examined, the latter through chemical and fusibility analyses of the ashes. Ahlada lignite (AL) was of low quality, with a calorific value of 8.9 MJ/kg. The biomass materials, ginning cotton waste (GCW) and pine needles (PN) had calorific values 16.6 MJ/kg and 20.1 MJ/kg, respectively. The slagging/fouling propensity of AL ash was low, whereas that of biomass wastes was medium to high. Thermal treatment of the samples and their blends prior to gasification produced upgraded fuels. A Boudourd reaction occurred above 750 °C. Gasification reactivity followed the order: GCW > PN > AL. AL/PN mixtures presented additivity effects; however, AL/GCW mixtures presented synergy effects. When the lignite was blended with the biochars studied, its conversion increased from 90% to 94.5% and its cold gas efficiency from 31.8% to 35%. Generated gas attained a heating value of about 12 MJ/m^3.

Keywords: co-gasification; lignite; biomass; reactivity; synergy; ash

Citation: Vamvuka, D.; Tsagris, G.; Loulashi, C. Co-Gasification Performance of Low-Quality Lignite with Woody Wastes Using Greenhouse Gas CO_2—A TG–MS Study. *Sustainability* **2023**, *15*, 9818. https://doi.org/10.3390/su15129818

Academic Editor: Dino Musmarra

Received: 5 May 2023
Revised: 12 June 2023
Accepted: 14 June 2023
Published: 20 June 2023

1. Introduction

Combustion of solid fuels for power generation creates air pollution and is responsible, to a great extent, for the greenhouse gas effect. On the other hand, gasification has been identified as an environmentally friendly process, with higher flexibility of feedstocks and end products [1–3]. The product gas of gasification is suitable as an energy source in internal combustion engines, turbines and solid oxide fuel cells, or as source of biofuels and value-added chemicals [3–7]. A two-step process, the first step being the thermal decomposition of the solid feedstock producing liquid and gaseous fuels [2,3,7,8] and the second step, the gasification of char, increases the reactivity of char and the purity of gas, and at the same time, eliminates operational tar problems during the utilization of gas, such as pipe clogging or corrosion [8,9]. The heat required for the second step can be provided by the pyrolysis-combustible products and the coupling of the process with a power plant.

When carbon dioxide from flue gas streams is used as the gasifying agent, the process provides a potential solution to the greenhouse gas problem and carbon dioxide sequestration [1,2,10]. Global net CO_2 emissions must be negative in order to reduce the greenhouse gas effect caused by atmospheric CO_2. This concept is often described as bioenergy with carbon capture and storage (BECSS). Among the various technologies investigated, such as chemical looping combustion of biomass, co-combustion of coal and biomass, synergy between biogas plant and biomass power plant and oxy-combustion with heat accumulation [11], gasification of biomass with carbon dioxide is considered a highly promising technology. The Boudouard reaction ($C + CO_2 \leftrightarrow 2CO$ $\Delta H = 172$ kJ/mol) is highly endothermic, and an efficient reductant combined with a strong thermodynamic driving force

is required to ensure irreversibility. However, at temperatures above 700 °C the equilibrium shifts towards the formation of CO. This reaction is very important for the gasification of carbonaceous materials, incorporating CO_2 into a valorization cycle for the production of marketable fuels, instead of capturing and sequestration [1,12].

The effectiveness of the gasification process is dependent on many different factors including feedstock properties, type, the concentration of the gasifying agent and operating conditions. A high temperature favors syngas production, while a high specific surface area and a more disordered aromatic structure of char, as well as the presence of alkali or alkaline earth compounds enhance its reactivity [2,3,13–17]. Inherent alkali in fuel ashes can serve as natural catalysts [2,4,14,18–21]; however, in appliances operating above 1000 °C, they can cause slagging/fouling problems, thus reducing the availability of the systems and increasing the energy cost [22–25].

Given the recent worldwide energy and climate crisis, global policies have set the targets for transition to a low-carbon economy by recycling and the reuse of wastes as energy sources, in the context of global sustainability goals, a circular economy and reduction of carbon footprints through the promotion of renewables [26]. The European Green Deal [26] and Agricultural and Renewables Policy [27–29] are based on decarbonized energy by 2050 and penetration of agricultural wastes in energy markets. The declining of fossil fuel reserves and the environmental restrictions associated with them have led to higher operating costs and lower consumption. Therefore, for power plants to maintain their sustainability, a greater operating flexibility is required. As such, the combined processing of fossil fuels with renewable sources of energy, such as organic wastes showing good synergy with current power plants [30], in a sustainable manner, reducing the potential of global warming, seems an attractive solution. Coal, the principal fossil fuel for electricity generation worldwide (about 40% of global power) [4,31], is the indigenous fuel of many countries. On the other hand, forest and agricultural wastes are readily available in large quantities in most countries. The availability of energy from forest wastes could vary from 10 to 16 EJ/y globally, while that from agricultural wastes could vary from 5 to 27 EJ/y [28].

The carbon dioxide gasification of high-rank coal, mainly of bituminous type, with agricultural residues including sorghum, rice straw, empty fruit bunches, walnut shells [14,18,19,32,33], or forest residues such as pine and oak wood [2,4], has been extensively studied. Past investigations have focused on interactions between fuels, catalytic effects of alkali metals [18,19,32,34] and kinetic analysis of the process [2,4,14,33]. There is limited information on the co-gasification of low-quality lignites with agricultural or forest waste (peanut shells, orange peel, soybean stalk, redwood) [34]. Lignite, which is an important fuel for several national economies around the world, has more proximity with biomass than high-rank coal, and its co-processing with various biomass materials to cover uncertainties in their availability could lead to different kinds of interactions. Therefore, the blending of these fuels for energy generation is challenging. Furthermore, there is lack of data on the characterization of all solid, liquid and gaseous products of the process and evaluation of their energy potential, or their deposition propensity with regard to fuel ashes.

Based on the previous analysis, this work aimed to investigate the carbon dioxide gasification performance of low-quality lignite-agro-industrial/forest waste blends, namely ginning cotton waste and pine needles, in terms of reactivity, conversion, cold gas efficiency, product gas composition and heating value. The experiments were conducted in a fixed bed unit and a thermal analysis mass spectrometer system. Raw materials, chars, liquids and gases were quantitatively analyzed and their energy content was determined. Synergetic effects and the role of minerals were examined, the latter through chemical and fusibility analyses of the ashes.

2. Materials and Methods

2.1. Raw Fuels and Characterization

One lignite and two biomass materials were selected for present study. The lignite (AL) was provided from the open-pit mine of Ahlada, located in Western Macedonia in

North Greece. Ginning cotton waste (GCW) was provided from a nearby enterprise and pine needles (PN) were collected from a local forest of the area. Samples were air-dried, riffled and ground to a final particle size below 200 μm (lignite in a jaw crusher and a ball mill, organic wastes in a cutting mill). Blends of lignite with each biomass material were also prepared at weight ratios of 70:30 and 50:50, respectively. These were chosen on the basis of typical ratios used in power plants co-processing such fuels [35], as well as on the low quality of lignite studied requiring a higher-grade material to improve its performance. Fuel characterization was performed in accordance with ASTM standards for the lignite (D5142, D5373, D4239, D5865) and European standards for the solid wastes (CEN/TC335).

Ashes were analyzed using an X-ray fluorescence spectrometer (S2 Ranger EDS, Bruker AXS) to determine their composition of inorganic elements, as well as a heating microscope with a high-definition video camera (Leitz Wetzlar EM201, Hesse Inst., Wetzlar, Germany) to determine their fusibility behavior. Deposition tendency was predicted through common slagging/fouling indices, calculated as follows:

Base-to-acid ratio (B/A) [23]:

$$B/A = \%(Fe_2O_2 + CaO + MgO + K_2O + Na_2O)/(SiO_2 + TiO_2 + Al_2O_3) \quad (1)$$

When B/A < 0.5 deposition tendency is low, when 0.5 < B/A < 1 deposition tendency is medium and when B/A > 1 deposition tendency is high.

Babcock index (Rs) [22]:

$$Rs = (B/A)S \quad (2)$$

where S is the percentage of sulphur in dry fuel.

When Rs < 0.6 deposition tendency is low, when 0.6 < Rs < 2 deposition tendency is medium, while when Rs > 2 deposition tendency is high.

Slag viscosity index (Sv) [22]:

$$Sv = SiO_2.100(SiO_2 + Fe_2O_2 + CaO + MgO) \quad (3)$$

If Sv > 72 slagging tendency is low, if 65 < Sv < 72 slagging tendency is medium and if Sv < 65 slagging tendency is high.

Ash fusibility index (Fs) [22]:

$$Fs = (4IDT + HT)/5 \quad (4)$$

Fusibility is low when Fs > 1342, medium when 1232 < Fs < 1342 and high when Fs < 1232.

Alkali index (AI) for biomass fuels [23]:

$$AI = kg\ (K_2O + Na_2O)/GJ \quad (5)$$

When AI = 0.17–0.34 kg/GJ deposition tendency is low, while when AI > 0.34 kg/GJ deposition tendency is high.

2.2. Char Production

For chars production, a lab-scale fixed-bed system was used (Figure 1), as previously described by the authors [8]. The stainless steel reactor (ID = 70 mm, H = 140 mm) was equipped with a stainless steel grid basket to support the sample, a Ni-Cr-Ni thermocouple in contact with the sample bed and a programmable high-temperature furnace with temperature controller of ±3 °C accuracy. After flushing with nitrogen to purge air, the sample was heated up to 600 °C with a rate of 10 °C/min, under a flow of nitrogen of 200 mL/min and retention time 30 min. Solid products of pyrolysis were analyzed with the same standard methods as for the raw fuels. The higher heating value (HHV) of liquid products, obtained after centrifugation of condensable volatiles, was determined by a bomb calorimeter (AC-300, Leco, St. Joseph, MI, USA), while the higher heating value of gases was calculated from the composition of gas and the higher heating values of

individual gases, derived after conducting TG–MS (thermogravimetric mass spectrometry) experiments using the same experimental conditions as those of the fixed-bed system. The average heating value of hydrocarbon species measured was 70 MJ/m^3. High-purity argon of flow rate 35 mL/min was used for these tests. The transfer line of product gases to the MS was a fused silicon capillary, which was insulated, heated and maintained at 200 °C to avoid species condensation. The secondary electron multiplier operated at 82 eV and 1–400 atomic mass and detected the ions which were separated according to their mass-to-charge ratio. Pyris v3.5 and Quadstar 422 software was used for acquisition of data. Calibration factors were determined from standard gases of high purity in argon. Description of the equipment (TG/DTG Perkin Elmer-MS/SEM QME-200, Balzers, Liechtenstein) and operating conditions can be found elsewhere [8].

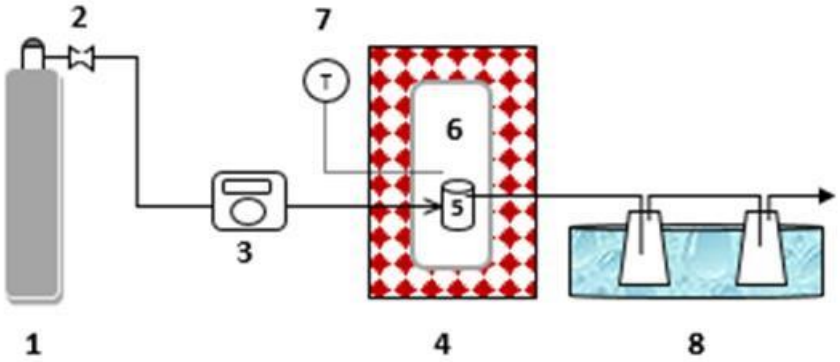

Figure 1. Diagram of fixed bed system: (1) N_2 cylinder, (2) flow control valve, (3) mass flow meter, (4) thermoprogrammable furnace, (5) sample, (6) reactor, (7) thermocouple with indicator and (8) ice baths.

2.3. Carbon Dioxide Gasification Experiments

For the gasification of chars and their mixtures in a carbon dioxide atmosphere, the thermal analysis system TG/DTG (sensitivity < 5 μg, temperature precision ±2 °C, balance accuracy 0.2% wt) was used. The weight loss of each sample and the derivative weight loss were measured continuously as functions of temperature from 25 °C up to 1000 °C. The heating rate was 10 °C/min, the flow rate of carbon dioxide 35 mL/min and the flow rate of nitrogen purge gas 45 mL/min. Analysis of gas was carried out using the mass spectrometer coupled online with the thermal analyzer, as mentioned above. Reproducibility of replicate tests was verified by the relative standard deviation (RSD).

The reactivity of each fuel was derived by the following equation:

$$R_G = \frac{R_{\max}}{T_{\max}} \times 100(1/\min{}^{\circ}\mathrm{C}) \quad (6)$$

where R_{max}, T_{max} the peak reaction rate and temperature, respectively.

Conversion efficiency (dry ash free %) was calculated by:

$$CE = \frac{m_g}{m_c} \times 100(\%) \quad (7)$$

where m_g and m_c the masses of gas and char, respectively.

The cold gas efficiency [3] was determined as follows:

$$CGE = \frac{m_g LHV_g}{m_c LHV_c} \times 100(\%) \quad (8)$$

where m_g, m_c are the masses of gas and char, respectively (kg), whereas LHV_g and LHV_c are the lower heating values of gas and char, respectively (MJ/kg).

3. Results and Discussion

3.1. Raw Fuel Characterization

Table 1, presenting the proximate and elemental analyses of the fuels studied, shows that AL was low-quality lignite, highly oxygenated and with a large amount of ash (35.8%), which lowered its calorific value. Its sulfur concentration was also considerable, revealing some emissions of sulfur compounds, such as H_2S, during gasification. On the other hand, both biomass fuels were rich in volatiles (~76–77%), had very low polluting sulfur and nitrogen content, a much smaller amount of ash (5.7–8.6%) and accordingly, an increased calorific value.

Table 1. Proximate and ultimate analysis of raw fuels (% dry).

Sample	Volatiles	Fixed Carbon	Ash	C	H	N	O	S	GCV * (MJ/kg)
AL	36.7	27.5	35.8	27.5	2.1	0.5	32.9	1.2	8.9
GCW	75.8	15.6	8.6	41.9	6.1	0.8	42.4	0.2	16.6
PN	76.8	17.5	5.7	47.8	6.9	0.2	39.3	0.05	20.1

* GCV: gross calorific value.

From the chemical analysis of ashes expressed as oxides in Figure 2, it can be observed that the ash of lignite contained a large amount of Si and a small amount of alkali Ca, Mg, K and Na, as opposed to the ash of biomass materials, which were rich in Ca, Mg, K and Na, especially the ash of GCW. These alkali metals are reported to present catalytic activity during the gasification process, while Si and Al are known to suppress the reaction rate [3,36].

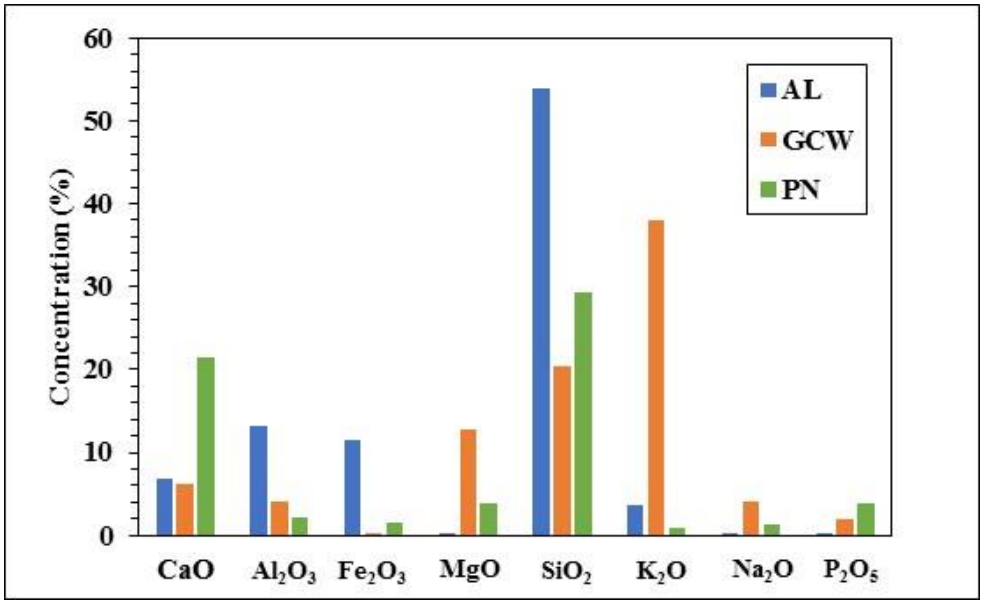

Figure 2. Chemical analysis of ashes of fuels.

The characteristic fusion temperatures of ash obtained by the heating microscope are compared in Figure 3. Initial deformation temperatures (IDT), ranging between 1050 °C and 1290 °C, are considered low for systems operating above 1000 °C, implying deposition problems. The fusion temperatures of lignite ash were much higher, reflecting its greater Si content, and lower in alkali species. Furthermore, it is interesting to note that GCW presented the lowest temperature difference between IDT and fluid (FT) temperatures, being known to induce a higher fouling rate in boilers [23].

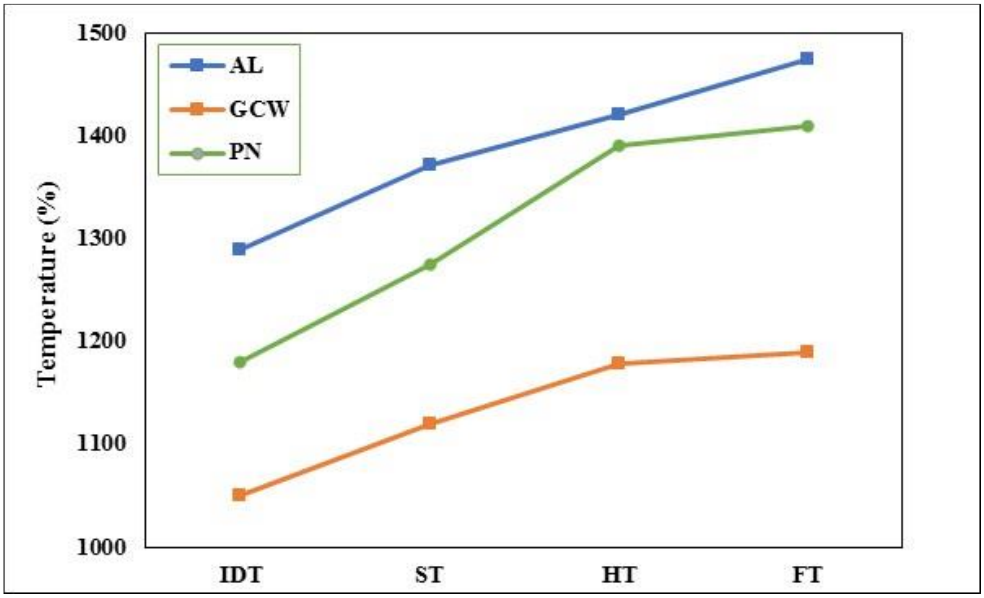

Figure 3. Characteristic fusion temperatures of ashes.

According to these results and the chemical analysis of ashes of mixtures (Table 2), the slagging/fouling indices of all fuels and lignite/biomass blends were calculated (Equations (1)–(5)) and included in Table 3. As can be seen, the deposition tendency of AL is predicted to be low; however, that of biomass wastes is medium to high. To keep the slagging/fouling propensity low to medium, the biomass percentage in the mixture should not exceed 30%.

Table 2. Chemical analysis of ashes of mixtures.

Sample		CaO	Al_2O_3	Fe_2O_3	MgO	SiO_2	K_2O	Na_2O	P_2O_5
AL/GCW	70:30	6.6	10.4	8.1	3.9	43.8	14.0	1.3	0.8
	50:50	6.5	8.6	5.8	6.4	37.1	20.9	2.0	1.1
AL/PN	70:30	11.2	9.9	8.6	1.2	46.4	2.9	0.4	1.4
	50:50	14.1	7.7	6.6	2.0	41.5	2.3	0.7	2.1

Table 3. Slagging/fouling indices of fuels and deposition tendency.

Sample		AI	B/A	R_s	S_v	F_s	Deposition Tendency
AL			0.32	0.38	74.4	1316	low
GCW		0.19	2.51	0.50	51.6	1076	high
PN		0.006	0.93	0.05	51.9	1222	medium to high
AL/GCW	70:30		0.70	0.63	69.6	1251	medium
	50:50		0.96	0.67	66.0	1200	medium
AL/PN	70:30		0.45	0.38	68.5	1296	low to medium
	50:50		0.55	0.34	64.1	1272	medium

3.2. Pyrolysis Products Characterization

The characterization of the solid products, after fuel devolatilization up to 600 °C, is presented in Table 4. Thermal decomposition resulted in the removal of H- and O- volatile compounds, leaving a char material enriched in carbon and mineral matter. The calorific value was increased in comparison to raw fuels and the higher value was obtained for GCW char. When AL lignite was mixed with the biomass materials, an upgraded char with higher organic matter and lower ash content was produced, resulting in an enhanced heating value.

Table 4. Proximate and ultimate analysis of chars (% dry).

Sample	Organic Matter	Ash	C	H	N	O	S	GCV (MJ/kg)
AL	48.2	51.8	38.7	1.3	0.5	6.4	1.3	14.3
GCW	73.1	26.9	65.3	1.9	0.7	5.2	-	23.9
PN	79.9	20.1	63.5	1.9	0.8	13.7	-	22.4
AL/GCW 70:30	55.0	45.0	46.5	1.6	0.5	5.4	1.0	17.4
50:50	60.9	39.1	52.4	1.6	0.6	5.5	0.8	19.3
AL/PN 70:30	58.1	41.9	46.3	1.4	0.5	9.0	0.9	16.9
50:50	64.6	35.4	51.5	1.6	0.6	10.2	0.7	18.5

The composition of the gaseous products of pyrolysis, as measured by the TG–MS system, is shown in Figure 4, whereas the higher heating values of chars, oils and gases from the fuels under study are compared in Figure 5. The principal constituents of evolved light gases were CO and CO_2, with lower quantities of CH_4, H_2 and C_xH_y, which were formed at higher temperatures, from the cracking of stronger aliphatic or aromatic bonds [37]. As seen in Figure 5, the higher heating value of PN gas was greater (13.4 MJ/m^3), due to its higher content in CO (~90%), satisfying the requirements in thermal energy for the process [8]. In addition, the calorific value and the yield of bio-oil produced from this fuel were the highest among the samples, reaching values 33.8 MJ/kg and 56.3%, respectively. Nevertheless, the calorific values of both GCW and PN bio-oils, ranging between 25 MJ/kg and 34 MJ/kg, were higher than values reported for other biomass materials [38].

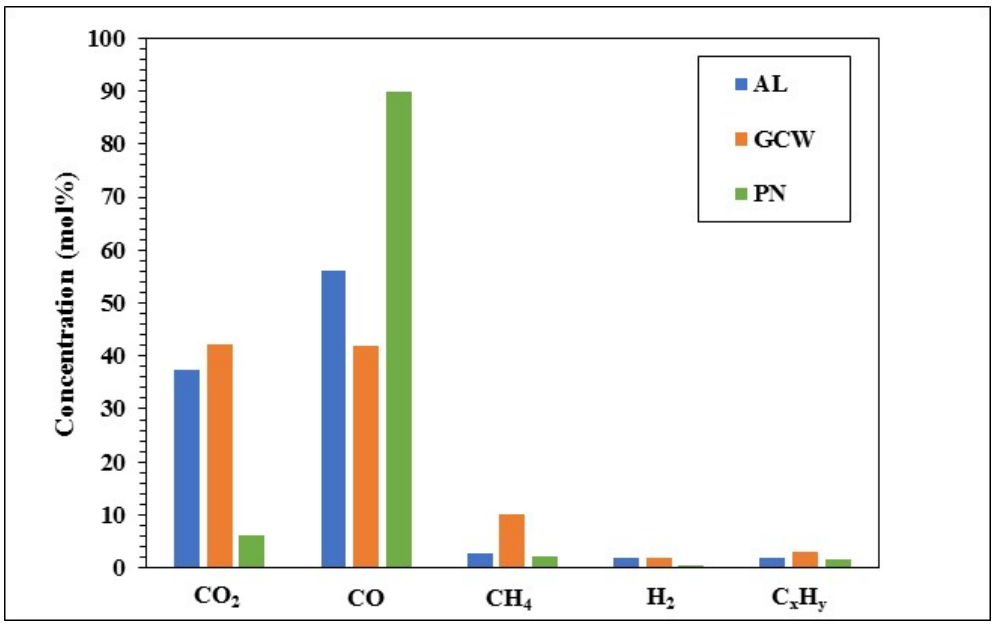

Figure 4. Composition of the gaseous products of pyrolysis of fuels.

3.3. Gasification Characteristics of Lignite and Biomass Chars and Their Mixture

Figure 6 compares the DTG (differential thermogravimetric) profiles of the lignite and the two biochar materials as a function of temperature and Table 5 summarizes the characteristic parameters derived from the processing of these curves, along with the average composition of product gas between 600 °C and 1000 °C and its higher heating value, for all fuels and blends studied. As can be observed, a Boudouard reaction occurred above 750 °C. GCW and PN biochars presented a peak inflection temperature around 890 °C and displayed a much higher rate than the lignite AL. The maximum rate of GCW was 2-fold higher than that of PN and about 6-fold higher than that of AL. The reactivity of fuels followed the order: GCW > PN > AL. Additionally, in the case of AL, the conversion of organic matter to gas was not complete and the cold gas efficiency was lower (31.8%) than the corresponding GCW and PN samples (41.2% and 40.1%), which is in agreement

with earlier data [10]. This low-reactivity behavior of AL char is associated with its high-ash content, richness in silicon and aluminum inhibitors to the gasifying agent, as shown in Figure 2. Accordingly, the conversion of AL lignite was reduced compared to the GCW and PN samples, whereas product gas composition was not affected by the mineral matter. On the other hand, the great reactivity of GCW char and consequently, the final conversion are correlated to its enhanced specific surface area (57.4 m^2/g) as also demonstrated by past investigations [1,15,36], as well as its high concentration in inherent alkali K and Na (Figure 2), which are known to exhibit a catalytic effect during gasification [1,14]. Finally, Table 5 shows that the higher heating value of generated gas was practically the same for all fuels, because the principal gas component was CO and it was higher in comparison to other gasification processes, such as those using steam as the gasifying agent. Previous research by the authors has shown that the higher heating value of gas generated by steam gasification of various biomass fuels varied between 9.6 MJ/m^3 and 11.4 MJ/m^3 [39]. The amounts of H_2, H_2O, CH_4 and C_xH_y were minor.

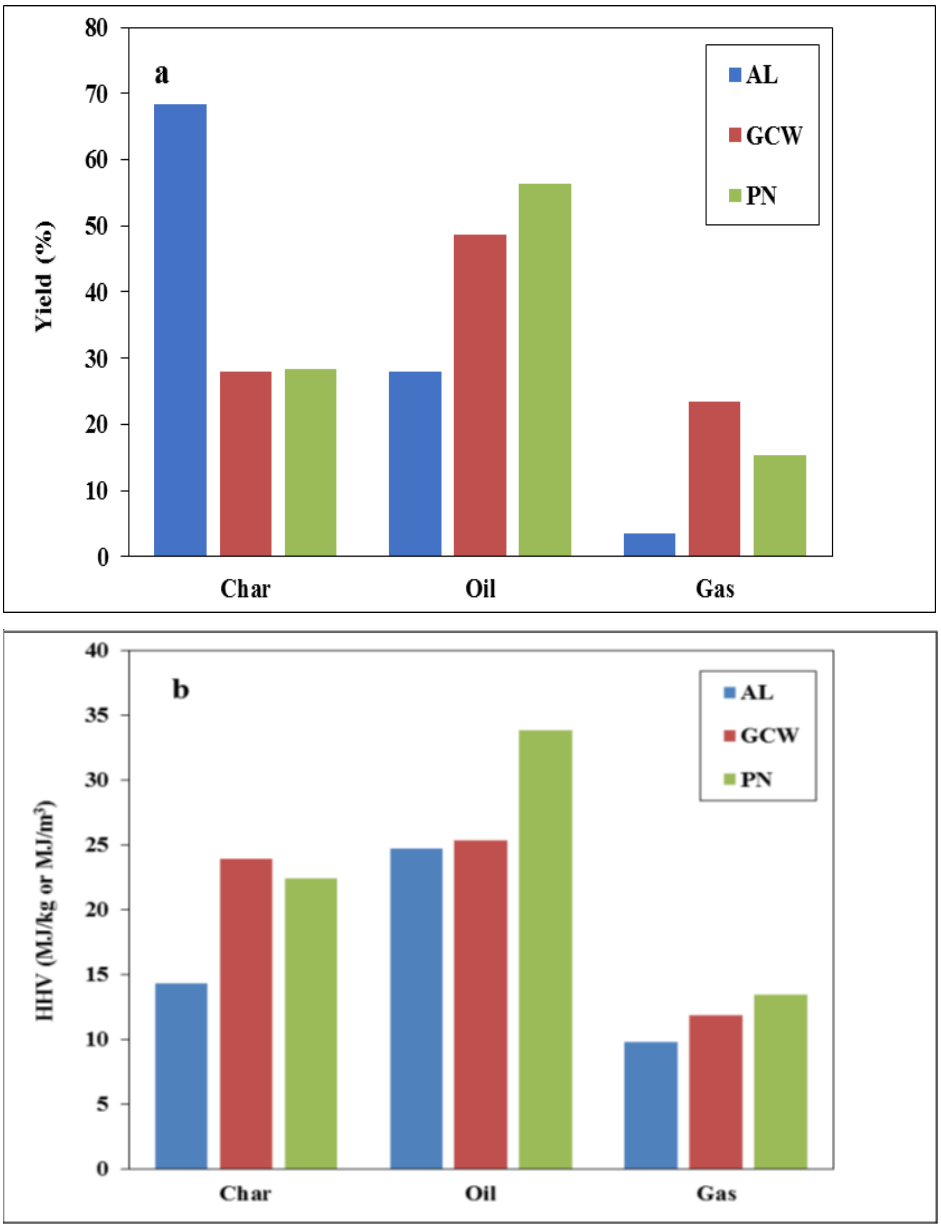

Figure 5. Yield (**a**) and higher heating values (**b**) of chars, oils and gases from the pyrolysis of fuels.

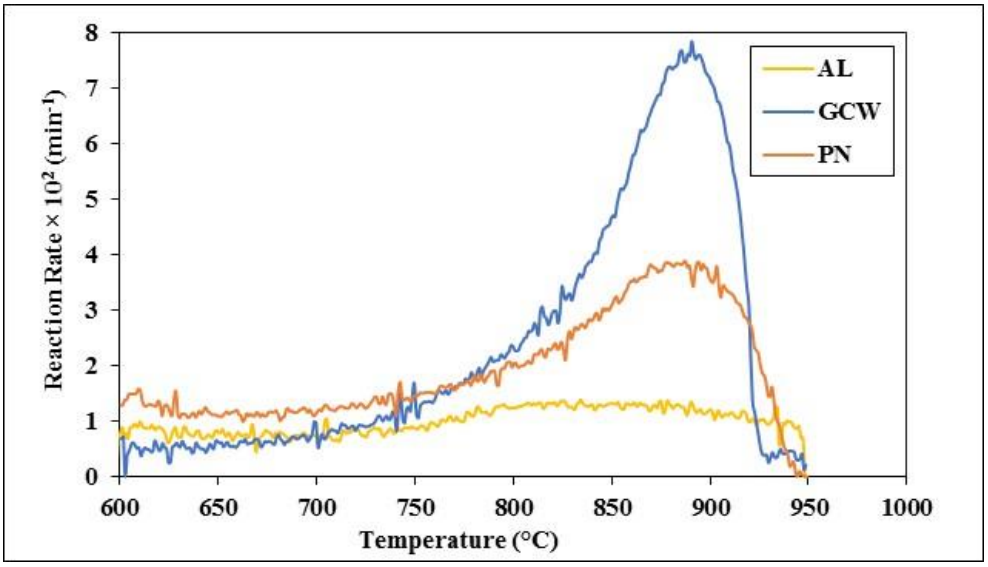

Figure 6. DTG profiles of the lignite and the two biomass materials (RSD = 0.3–0.5%).

Table 5. Gasification parameters of fuels and blends (dry basis).

Sample		AL	GCW	PN	AL/GCW 70:30	AL/GCW 50:50	AL/PN 70:30	AL/PN 50:50
T_{max} (°C)		860	893	890	923	937	910	917
$R_{max} \times 10^2$ (min^{-1})		1.4	8.0	3.9	1.7	2.0	2.0	2.4
$R_G \times 10^4$ (min^{-1}/°C)		0.16	0.89	0.44	0.19	0.21	0.22	0.26
Gas (mol%)	CO	93.4	92.3	92.2	93.2	92.9	93.1	93.0
	H_2O	5.0	5.9	6.3	5.1	5.3	5.3	5.5
	H_2	1.3	1.5	1.1	1.4	1.5	1.3	1.2
	CH_4	0.1	0.08	0.1	0.1	0.1	0.1	0.1
	C_xH_y	0.2	0.2	0.2	0.2	0.2	0.2	0.2
HHV (MJ/m^3)		12.2	12.1	12.0	12.2	12.1	12.1	12.1
CE (%)		90.0	100.0	100.0	92.4	94.1	92.0	94.5
CGE (%)		31.8	41.2	40.1	30.9	31.5	33.6	35.0

Upon the gasification of coals with biomass materials, synergistic effects are known to take place, when different results are obtained in comparison to those achieved from the weighted average values of the individual fuel components [4,19,34]. These mutual interactions are the result of several complex mechanisms and are favored when the fuels react in the same temperature regime. Blends of feed ratio, gasifying agent, temperature, physical structure and chemical composition of component fuels are the important controlling parameters [20]. During current experiments, it was observed that when the lignite was mixed with the biomass materials at percentages up to 50%, the gasification behavior of the GCW and PN mixtures was different. From Table 5 and Figures 6 and 7, it can be seen that the characteristic parameters of the AL/PN mixtures, such as reaction rate and reactivity, were very close to the weighted average values, implying additivity effects between component fuels. However, for AL/GCW blends, peak position was displayed at a higher temperature than the theoretically expected value and reaction rate and reactivity were much lower than expected from the contribution of each fuel, suggesting synergy effects between AL and GCW materials. Taking into consideration that operating conditions, reaction regime and blending ratios were the same for the chars studied, the reasons behind the behavior of AL/GCW mixtures could be found in the structure and composition of the fuels. Although the higher specific surface area of GCW and its high content in K and Na which exhibited a catalytic effect, as previously shown, were expected to significantly increase the reactivity of the blends, this was only slightly improved and did not show a linear relationship with the amount of blending. It is possible that the increased percentage of silicon and aluminum

of lignite ash had a negative effect on alkali catalysts, due to blocking of the metals by forming aluminosilicates, as reported by some previous studies [1,20,34]. Additionally, the O/C molar ratio of AL–GCW char blends (Table 4) was much lower (0.07–0.09) than that of AL–PN blends (0.14–0.15) or the lignite (0.12), indicating a more ordered aromatic structure with greater stability [3], leading to reduced reactivity. Further investigations are needed to provide some insights into such synergistic mechanisms.

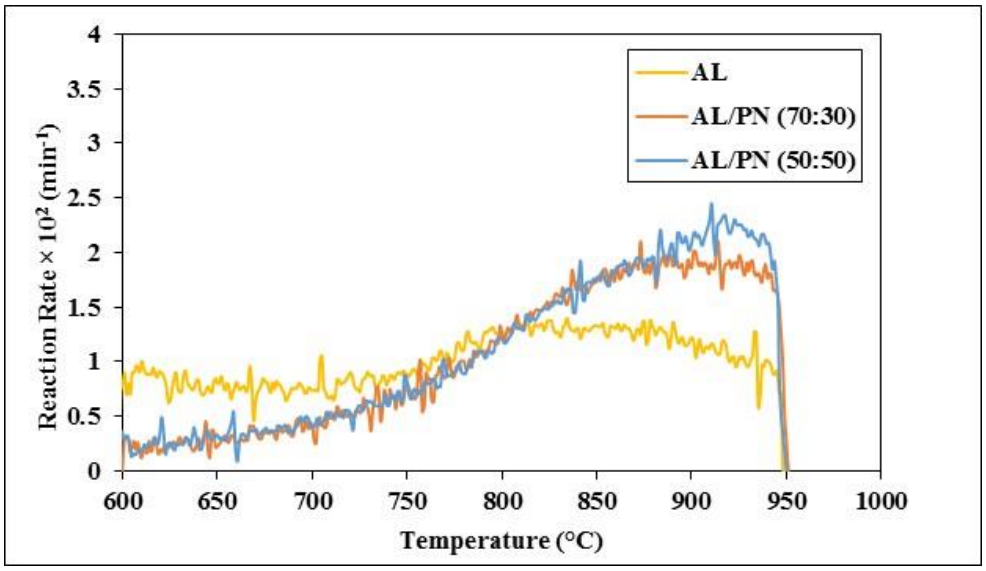

Figure 7. DTG profiles of the lignite-biomass blends (RSD = 0.5–0.7%).

Nevertheless, the upgraded chars produced after blending lignite with the biomass fuels and pyrolyzing at 600 °C, having higher organic matter and lower ash than the lignite, presented increased gasification reactivity and enhanced conversion. Additionally, the cold gas efficiency was increased from 31.8% (for lignite) to 35% (blends), mainly due to the larger amount of gas produced, whereas the higher heating value of product gas reflected the higher heating value of CO too, for all mixtures. Generated CO gas can be utilized as a fuel for industrial combustion purposes, or as a reagent for the production of hydrogen via the water–gas shift reaction, of methanol by catalytic processes, of liquid fuels via Fischer–Tropsch synthesis and of various chemicals [1,12,40].

4. Conclusions

AL lignite, having a high amount of ash (35.8%), was of low quality, with a calorific value 8.9 MJ/kg. Biomass materials, GCW and PN, were rich in volatiles and their calorific values were 16.6 MJ/kg and 20.1 MJ/kg, respectively. The slagging/fouling propensity of AL ash was low, whereas that of biomass wastes was medium to high.

Thermal treatment of the samples and their blends prior to gasification produced upgraded fuels in comparison to raw materials. The higher heating value of solid, liquid and gaseous products of this process varied between 14.3–23.9 MJ/kg, 24.7–33.8 MJ/kg and 9.8–13.4 MJ/m^3, respectively.

A Boudouard reaction occurred above 750 °C. The maximum rate of GCW was 2-fold higher than that of PN and about 6-fold higher than that of AL. Gasification reactivity followed the order: GCW > PN > AL. AL/PN mixtures presented additivity effects, however AL/GCW mixtures presented synergy effects. When the lignite was blended with the biochars studied, its conversion increased from 90% to 94.5% and its cold gas efficiency from 31.8% to 35%. The generated gas attained a heating value of 12–12.2 MJ/m^3, as CO was the main component.

Author Contributions: Conceptualization, D.V.; methodology, D.V.; software, G.T. and C.L.; validation, D.V.; investigation, D.V.; data curation, G.T. and C.L.; writing—original draft preparation, D.V.; writing—review and editing, D.V. All authors have read and agreed to the published version of the manuscript.

Funding: This research received no external funding.

Institutional Review Board Statement: Not applicable.

Informed Consent Statement: Not applicable.

Data Availability Statement: Not applicable.

Acknowledgments: The authors kindly thank the laboratories of Hydrocarbons Chemistry and Technology, Geochemistry and Applied Mineralogy of the Technical University of Crete for the ultimate analysis and ash analyses of the samples.

Conflicts of Interest: The authors declare no conflict of interest.

References

1. Lahijani, P.; Zainal, Z.; Mohammadi, M.; Mohamed, A. Conversion of the greenhouse gas CO_2 to the fuel gas CO via the Boudouard reaction: A review. *Renew. Sustain. Energy Rev.* **2015**, *41*, 615–632. [CrossRef]
2. Beagle, E.; Wang, Y.; Bell, D.; Belmont, E. Co-gasification of pine and oak biochar with sub-bituminous coal in carbon dioxide. *Bioresour. Technol.* **2018**, *251*, 31–39. [CrossRef] [PubMed]
3. Vamvuka, D.; Teftiki, A.; Sfakiotakis, S. Increasing the reactivity of waste biochars during their co-gasification with carbon dioxide using catalysts and bio-oils. *Thermochim. Acta* **2021**, *704*, 179015. [CrossRef]
4. Masnadi, M.; Grace, J.; Bi, X.; Lim, C.; Ellis, N. From fossil fuels towards renewable: Inhibitory and catalytic effects on carbon thermochemical conversion during co-gasification of biomass with fossil fuels. *Appl. Energy* **2015**, *140*, 196–209. [CrossRef]
5. Wu, H.; Xiao, J.; Zeng, X.; Li, X.; Yang, J.; Zou, Y.; Liu, S.; Dong, P.; Zhang, Y.; Liu, J. A high performance direct carbon solid oxide fuel cell-a green pathway for brown coal utilization. *Appl. Energy* **2019**, *248*, 679–687. [CrossRef]
6. Santos, R.G.; Alencar, A.C. Biomass-derived syngas production via gasification process and its catalytic conversion into fuels by Fischer Tropsch synthesis: A review. *Int. J. Hydrogen Energy* **2020**, *45*, 18114–18132. [CrossRef]
7. Lampropoulos, A.; Kaklidis, N.; Athanasiou, C.; Montes-Moran, M.A.; Arenillas, A.; Menendez, J.A.; Binas, V.D.; Konsolakis, M.; Marnellos, G.E. Effect of olive kernel treatment (torrefaction vs. slow pyrolysis) on the physicochemical characteritics and the CO_2 or H_2O gasification performance of as-prepared biochars. *Int. J. Hydrog. Prod.* **2021**, *46*, 29126–29141. [CrossRef]
8. Vamvuka, D.; Sfakiotakis, S.; Pantelaki, O. Evaluation of gaseous and solid products from the pyrolysis of waste biomass blends for energetic and environmental applications. *Fuel* **2019**, *236*, 574–582. [CrossRef]
9. Prasertcharoensuk, P.; Bull, S.J.; Phan, A.N. Gasification of waste biomass for hydrogen production: Effects of pyrolysis parameters. *Renew. Energy* **2019**, *143*, 112–120. [CrossRef]
10. Zheng, X.; Ying, Z.; Wang, B.; Chen, C. Hydrogen and syngas production from municipal solid waste (MSW) gasification via reusing CO_2. *Appl. Therm. Eng.* **2018**, *144*, 242–247. [CrossRef]
11. Ziolkowski, P.; Madejski, P.; Amiri, M.; Kus, T.; Stasiak, K.; Subramanian, N.; Pawlak-Kruczek, H.; Badur, J.; Niedźwiecki, L.; Mikielewicz, D. Thermodynamic analysis of negative CO_2 emission power plant using Aspen plus, Aspen hysys and Ebsilon software. *Energies* **2021**, *14*, 6304. [CrossRef]
12. Chan, Y.H.; Rahman, S.N.F.S.A.; Lahuri, H.M.; Khalid, A. Recent progress on CO-rich syngas production via CO_2 gasification of various wastes: A critical review on efficiency, challenges and outlook. *Environ. Poll.* **2021**, *278*, 116843. [CrossRef] [PubMed]
13. Guizani, C.; Haddad, K.; Jeguirim, M.; Colin, B.; Limousy, L. Combustion characteristics and kinetics of torrefied olive pomace. *Energy* **2016**, *107*, 453–463. [CrossRef]
14. Mafu, L.; Neomagus, H.; Everson, R.; Okolo, G.; Strydom, C.; Bunt, J. The carbon dioxide gasification characteristics of biomass char samples and their effect on coal gasification reactivity during co-gasification. *Bioresour. Technol.* **2018**, *258*, 70–78. [CrossRef]
15. Eshun, J.; Wang, L.; Ansah, E.; Shahbazi, A.; Schimmel, K.; Kabadi, V.; Aravamudhan, S. Characterization of the physicochemical and structural evolution of biomass particles during combined pyrolysis and CO_2 gasification. *J. Energy Inst.* **2019**, *92*, 82–93. [CrossRef]
16. Maya, J.C.; Macias, R.; Gomez, C.A.; Chejne, F. On the evolution of pore microstructure during coal char activation with steam/CO_2 mixtures. *Carbon* **2020**, *158*, 121–130. [CrossRef]
17. Wang, M.; Wan, Y.; Guo, Q.; Bai, Y.; Yu, G.; Liu, Y.; Zhang, H.; Zhang, S.; Wei, J. Brief review on petroleum coke and biomass/coal co-gasification: Syngas production, reactivity characteristics and synergy behavior. *Fuel* **2021**, *304*, 121517. [CrossRef]
18. Naidu, V.; Aghalayam, P.; Jayanti, S. Synergetic and inhibition effects in carbon dioxide gasification of blends of coals and biomass fuels of Indian origin. *Bioresour. Technol.* **2016**, *209*, 157–165. [CrossRef]
19. Wei, J.; Gong, Y.; Guo, Q.; Chen, X.; Ding, L.; Yu, G. A mechanism investigation of synergy behavior variations during blended char co-gasification of biomass and different rank coals. *Renew. Energy* **2018**, *131*, 597–605. [CrossRef]

20. Abdalazeez, A.; Li, T.; Wang, W.; Abuelgasim, S. A brief review of CO_2 utilization for alkali carbonate gasification and biomass/coal co-gasification: Reactivity, products and process. *J. CO_2 Utiliz.* **2021**, *43*, 101370. [CrossRef]
21. Yang, P.; Zhao, S.; Zhang, Q.; Hu, J.; Liu, R.; Huang, Z.; Gao, Y. Synergetic effect of the cotton stalk and high-ash coal on gas production during co-pyrolysis/gasification. *Bioresour. Technol.* **2021**, *336*, 125336. [CrossRef] [PubMed]
22. Garcia-Maraver, A.; Mata-Sanchez, J.; Carpio, M.; Perez-Jimenez, J. Critical review of predictive coefficients for biomass ash deposition tendency. *J. Energy Inst.* **2017**, *90*, 214–228. [CrossRef]
23. Vamvuka, D.; Sfakiotakis, S.; Mpoumpouris, A. Slagging and fouling propensities of ashes from urban and industrial wastes. *Rec. Innov. Chem. Eng.* **2018**, *11*, 145–158. [CrossRef]
24. Yao, X.; Zhou, H.; Xu, K.; Xu, Q.; Li, L. Evaluation of the fusion and agglomeration properties of ashes from combustion of biomass, coal and their mixtures and the effects of K_2CO_3 additives. *Fuel* **2019**, *255*, 115829. [CrossRef]
25. Wei, J.; Wang, M.; Xu, D.; Shi, L.; Li, B.; Bai, Y.; Yu, G.; Bao, W.; Fu, J.; Zhang, H.; et al. Migration and transformation of alkali/alkaline earth metal species during biomass and coal co-gasification: A review. *Fuel Process. Technol.* **2022**, *235*, 107376. [CrossRef]
26. Mulvaney, D. Green new deal. In *Sol Power*; University of California Press: Berkley, CA, USA, 2019.
27. Directive 2008/98/EC of the European Parliament and of the Council of 19 November 2008, on waste and repealing certain Directives. *OJL* **2008**, *312*, 3–30.
28. Vamvuka, D. *Biomass, Bioenergy and the Environment*; Tziolas Publications: Salonica, Greece, 2009.
29. European Association for Coal and Lignite—Eurocoal. Eurocoal Market. 2019. Available online: http://www.eurocoal.eu (accessed on 1 November 2022).
30. REN21 Renewables 2020. Global Status Report. REN21 Secretariat: Paris, France. 2020. Available online: http://www.ren21.net/wp-content/uploads/2019/05/gsr_2020_full_report_en.pdf (accessed on 15 November 2021).
31. International Energy Agency. Coal. 2018. Available online: http://www.iea.org/16topics/coal/ (accessed on 1 December 2020).
32. Parvez, A.M.; Mujtaba, I.M.; Pang, C.; Lester, E.; Wu, T. Effect of the addition of different waste carbonaceous materials on coal gasification in CO_2 atmosphere. *Fuel Process. Technol.* **2016**, *149*, 231–238. [CrossRef]
33. Diao, R.; Li, S.; Deng, J.; Zhu, X. Interaction and kinetic analysis of co-gasification of bituminous coal with wasnut shell under CO_2 atmosphere: Effect of inorganics and carbon structures. *Renew. Energy* **2021**, *173*, 177–187. [CrossRef]
34. Zhang, Y.; Zheng, Y.; Yang, M.; Song, Y. Effect of fuel origin on synergy during co-gasification of biomass and coal in CO_2. *Bioresour. Technol.* **2016**, *200*, 789–794. [CrossRef]
35. Roni, M.S.; Chowdhury, S.; Mamun, S.; Marufuzzaman, M.; Lein, W.; Johnson, S. Biomass co-firing technology with policies and challenges and opportunities: A global review. *Renew. Sustain. Energy Rev.* **2017**, *78*, 1089–1101. [CrossRef]
36. Li, R.; Zhang, J.; Wang, G.; Ning, X.; Wang, H.; Wang, P. Study on CO_2 gasification reactivity of biomass char derived from high-temperature rapid pyrolysis. *Appl. Therm. Eng.* **2017**, *121*, 1022–1031. [CrossRef]
37. Jayaraman, K.; Gokalp, I.; Petrus, S.; Belandria, V.; Bostyn, S. Energy recovery analysis from sugar cane bagasse pyrolysis and gasification using thermogravimetry, mass spectrometry and kinetic models. *J. Anal. Appl. Pyrolysis* **2018**, *132*, 225–236. [CrossRef]
38. Kim, K.H.; Kim, T.S.; Lee, S.M.; Choi, D.; Yeo, H.; Choi, I.G.; Choi, J.W. Comparison of physicochemical features of biooils and biochars produced from various woody biomasses by fast pyrolysis. *Renew. Energy* **2013**, *50*, 188–195. [CrossRef]
39. Vamvuka, D.; Afthentopoulos, E.; Sfakiotakis, S. H_2-rich gas production from steam gasification of a winery waste and its blends with industrial wastes. Effect of operating parameters on gas quality and efficiency. *Renew. Energy* **2022**, *197*, 1224–1232. [CrossRef]
40. Roncancio, R.; Gore, J.P. CO_2 char gasification: A systematic review from 2014 to 2020. *Energy Convers. Manag.* **2021**, *10*, 100060. [CrossRef]